Experimental and Numerical Analysis of Spalling Effect in TRC Specimens*

Jakub Jerabek[1], Allessandra Keil[2], Jens Schoene[3],
Rostislav Chudoba[4], Josef Hegger[5], Michael Raupach[6]

Abstract: The paper presents the study of spalling effect occurring under tensile loading in thin-walled TRC specimens. The experimentally observed failure patterns are first classified and the performed experiment design is explained and discussed. A parameter study of spalling effect with varied thickness of concrete cover and reinforcement configurations including both the textile fabrics and the yarns provided the basis for numerical analysis of the effect. The applied numerical model was designed in order to capture the initiation and propagation of longitudinal cracks leading to the separation of concrete blocks from the textile fabrics. A meso-scopic material resolution in a single crack bridge is used for the simulation exploiting the periodic structure of the crack bridges both in the lateral and in the longitudinal direction of the TRC specimens. The matrix was modeled using an anisotropic damage model falling in the microplane-category of material models. The bond between yarn and matrix follows a non-linear bond-law calibrated using pull-out tests. The epoxy-impregnated reinforcement is considered as a homogeneous bar.

1 Introduction

Recent experimental studies revealed that textile-reinforced concrete specimens produced using the standard AR-glass rovings exhibit low efficiency and achieve at most half of the theoretical yarn strength [1]. Due to the poor penetration of the cementious matrix, the contact area to the glass roving is relatively small. A high fraction of inner filaments has low or no contact to the matrix and does not contribute to the overall crack bridging force.

* This is a peer-reviewed paper. Online available: urn:nbn:de:bsz:14-ds-1244046893347-05461
[1] Dipl.-Ing.; Lehrstuhl und Institut für Massivbau; RWTH Aachen
[2] Dipl.-Ing.; Institut für Bauforschung; RWTH Aachen
[3] Dipl.-Ing.; Institut für Schweißtechnik und Fügetechnik; RWTH Aachen
[4] Dr.-Ing.; Lehrstuhl und Institut für Massivbau; RWTH Aachen
[5] Prof. Dr.-Ing.; Lehrstuhl und Institut für Massivbau; RWTH Aachen
[6] Prof. Dr.-Ing.; Institut für Bauforschung; RWTH Aachen

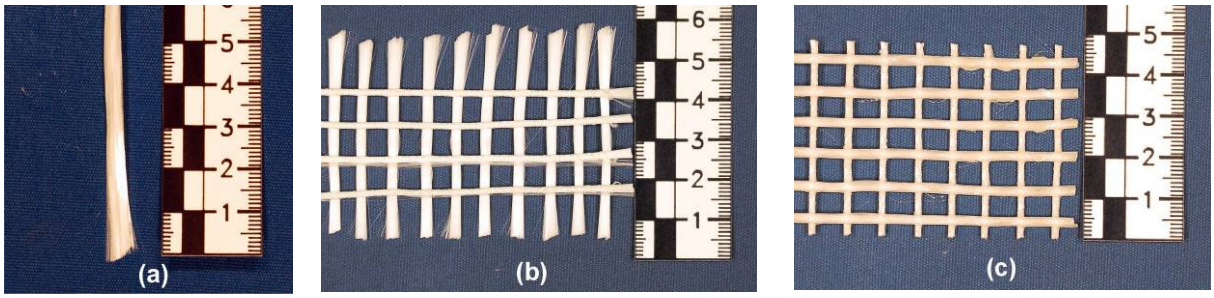

Fig. 1: (a) AR-glass roving 2400 tex, (b) glass fibre textile 2D-11-07, (c) glass fibre textile 2D-11 07 impregnated with epoxy

As shown experimentally in [2] penetration of the textile structures with high-modulus polymers can significantly increase the load-bearing capacities of TRC-components. The enhancement of the mechanical performance is accompanied with an altered failure pattern, which has not been observed for non-impregnated textile fabrics. Starting at a tensile load level of about 1000 N/mm² longitudinal cracks develop which cause in combination with the existing transverse cracks spalling of large dimensions. So far, the major factors affecting the spalling were investigated insufficiently. By reducing the danger of spalling the performance and safety of the TRC component especially under complex loads could be significantly increased.

The first step in the present study was to classify and characterize the spalling effects experimentally using component tests (tensile and bending tests) accompanied with the temporally and spatially resolved recording of crack development, particularly of longitudinal cracks. In addition, the stress- strain response was measured and the load level initiating longitudinal cracks has been determined. The experimental work including the applied materials, test setup and test results are described in Sec. 2.

In a second step the experimental experience was used in the development of the model that would reproduce the initiation of longitudinal cracks leading to spalling. The structure of the model and discussion of its feasibility is performed in Sec. 3.

2 Experimental and study of the spalling effect

2.1 Materials

2.1.1 Rovings and textiles

Rovings (yarns) of technical textiles consist of several hundred to several thousands of separate filaments with diameters of a few μm. The filaments are manufactured by use of the nozle pulling procedure. After their production the filaments are sized with a blend of

organic compounds. The size consists of a mixture of film formers, adhesives and antistatica [3] and facilitates subsequent processing of the glass fibers and reduces damage during production. Subsequently, the yarn is processed usually into two- or three-dimensional textiles fabrics like the one depicted in Fig. 1.

In the present study alkali resistant (AR-) glass rovings with a size produced by the Company OCV are used (VET-RO-ARG-2400-1-05). These rovings consist of approximately 1560 filaments with an average diameter of 27 μm, corresponding to a linear density of 2400 tex (1tex = 1g/km).

2.1.2 Polymers for roving impregnation

The purpose of roving impregnation with polymers is the improvement of the load-bearing capacity of textile reinforced concrete as well as an increase of its durability. Therefore, different types of polymers, primarily polymer dispersions and epoxies, were used for roving impregnation in previous investigations. These investigations showed that a maximum increase of the load-bearing capacity can be achieved using high modulus epoxies for roving impregnation [3]. Based on these results an ambient cured epoxy system (EP STF STD) has been chosen for roving and textile impregnation in this paper. This epoxy system is based on a bisphenol A-epichlorhydrin resin, which was cured by addition of an amine hardener according to the stoichiometric ratio. Prior to the embedding of the impregnated reinforcement into the concrete matrix, the impregnated rovings/textiles were stored under laboratory conditions (24h at 23°C / 50% r. h.).

2.1.3 Concrete

Within the scope of the SFB 532 a fine grained concrete denoted as PZ-0899-01 has been developed at the Institute für Bauforschung RWTH. In order to achieve a good bond, a high floating ability and small size of aggregate (max.: 0.6 mm) are required. The composition of PZ-0899-01 is summarized in Table 1. The mechanical properties are described in [4].

Table 1: Composition of fine grained concrete PZ 0899-01

Name	Cement (CEM I 52.5 R)	Fly ash (fa)	Silica fume (sf)	Sand < 0.6 mm	Quartz flour	Super-plastiziser	w/b = w/(c+fa+sf)
[-]	kg/m³	kg/m³	kg/m³	kg/m³	kg/m³	$\%\Sigma_{c+fa+sf}$	[-]
PZ 0899-01	490	175	35	714	499	1.5	0,4

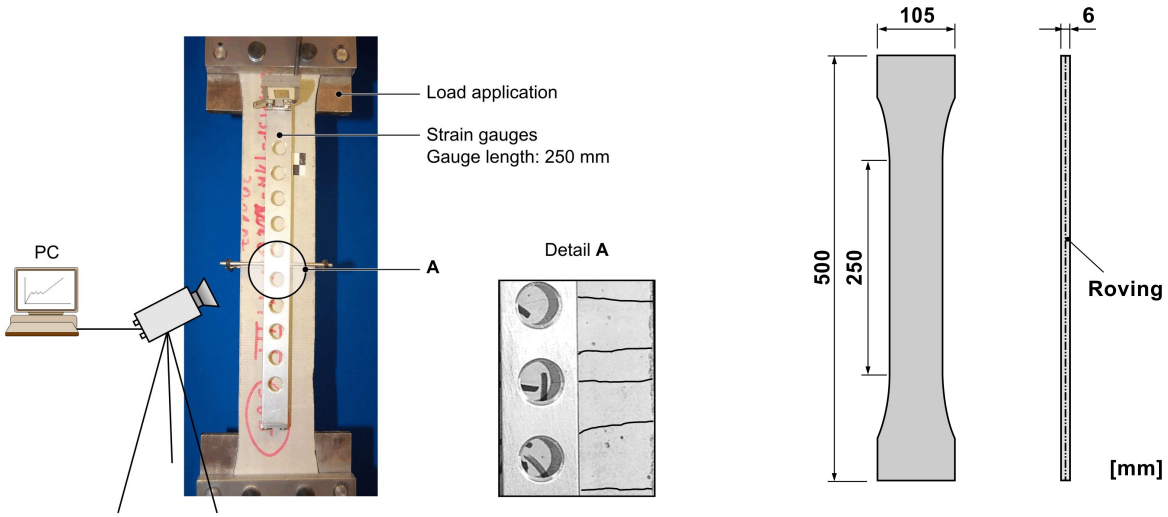

Fig. 2: Experimental setup of the TSP-test (left) and TSP-specimen (right)

2.2 Experimental program

The dog-bone shaped specimens (further referred to as TSP-specimens) have been produced. Either several detached rovings or a strip of the glass fiber textile are clamped centrally in a steel mold (500 • 105 • 6 mm³) and embedded in the fine concrete mixture PZ-0899-01. For these investigations non-impregnated and impregnated reinforcement was used. The samples were stored for 28 days at 23 °C and 95 % r. h. and then 7 days at 23 °C and 50 % r. h. The geometry of the TSP specimens is illustrated in Fig. 2 (right).

The specimens were produced and tested in a displacement-controlled testing device. The tensile load was applied via rounded off steel elements at a loading speed of 0.5 mm/min. During the testing the change of length was measured on two sides over 250 mm using electrical strain gauges. In the central area, the specimen width is constantly 60 mm over a length of 250 mm. This leads to a uniform stress distribution in the middle part of the specimen. The experimental setup of the TSP-test is shown in Fig. 2 (left).

After the curing of the concrete matrix the composite specimens were subjected to the TSP-test. The material compositions and parameters applied in the performed series are summarized in Table 2. Three specimen replications were tested in each series. The recorded response included the stress-strain curves and, at the same time, the monitoring of crack development and failure pattern during the loading by the use of a digital camera. Pictures of the crack pattern were taken at each 0.5 kN.

Table 2: Specification of the experimental program

Series No.	Type of reinforcement	Impregnation material	Thickness of the TSP specimens	Number of textile layers	Number of rovings in loading d.	Filament cross-section
[-]	[-]	[-]	mm	[-]	[-]	[mm²]
1	Textile 2D-11-07	-	10	2	12	10,7
2	Textile 2D-11-07	EP STF STD	10	1	6	5,3
3	Rovings of 2D-11-07	EP STF STD	10	1	6	5,3
4	Rovings of 2D-11-07	-	6	1	8	7,1
5	Rovings of 2D-11-07	EP STF STD	6	1	8	7,1

2.3 Discussion of test results

From experimentally measured load-displacement curves, nominal fiber stress-strain curves have been determined. Typical stress-elongation curves of the TSP-tests are given in Fig. 3(a). The nominal fiber stress has been simply calculated by dividing the applied force by the total filament cross-section. The tensile stress-strain behavior of TRC composites reinforced with non-impregnated glass fibers has already been studied in previous publications [5, 6]. The series 1 and 4 were mainly included for the matter of comparison.

As already mentioned, the impregnation leads to an improved efficiency of the mechanical properties of the reinforcement (Fig. 3(a)) [2]. At the same time, a different failure mechanism occurs starting at a load level (approx. 1000 N/mm²), which has not been attained by the use of non-impregnated reinforcement. After the multiple cracking of the matrix is completed (cracks in orthogonal direction) the formation of longitudinal cracks can be observed as it is shown in Fig. 3(b).

The crack formation mostly starts at the vicinity of a horizontal crack in the axes of the reinforcement. The crack development is frequently initiated in zones with visible initial imperfection (e.g. reinforcement apparent on the surface). With an increasing external load the crack extends further on. The failure is characterized by the splitting of the concrete cover along the axis of the reinforcement resulting frequently in the spalling of concrete next to the outmost yarn. The failure of the yarn usually follows immediately after the spalling of the concrete. In comparison to that the failure of a TSP specimen reinforced with non-impregnated rovings is characterized by the rupture of the yarn without the occurrence of a spalling effect.

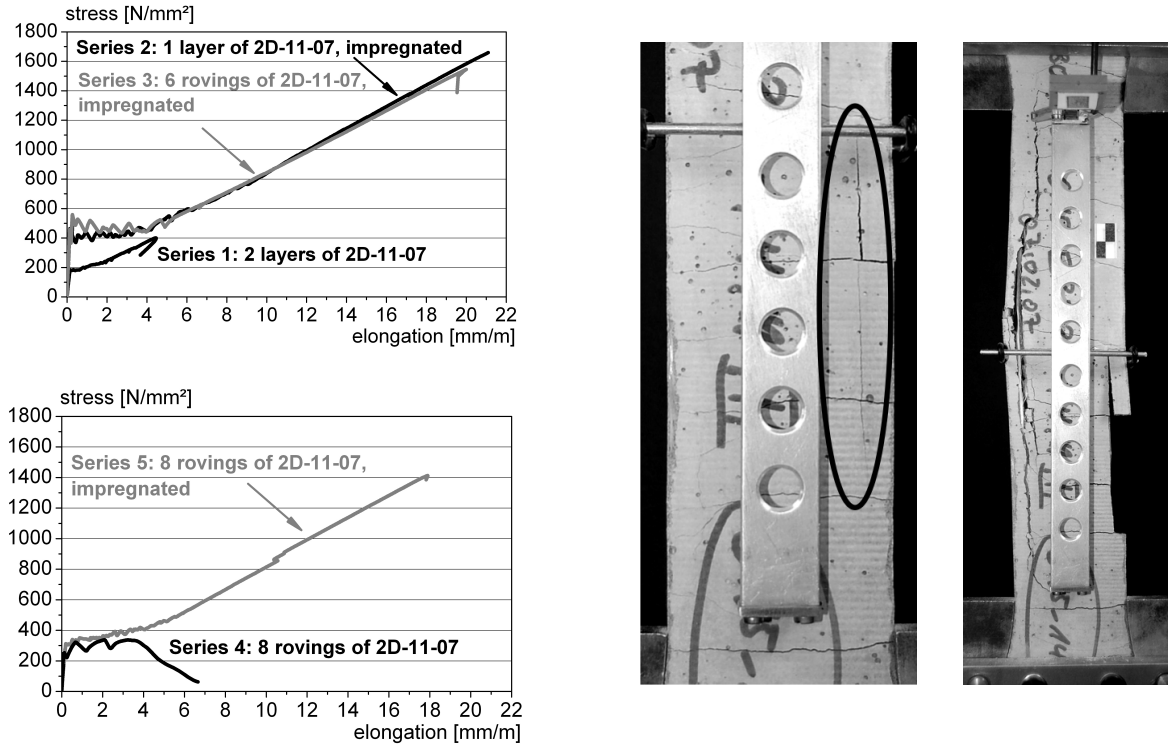

Fig. 3: (a) Nominal fiber stress-elongation curves determined with the TSP-test Discussion of test results (b) Observed crack pattern (left) state of failure (right) series 5 with the thickness 10mm.

In order to investigate the influence of the thickness of the concrete cover on the spalling behavior, TSP specimens with a thickness of 6 mm and 10 mm were produced and tested (see series 3 and 5). The failure progress of these two series seems to take place in a similar way (see Fig. 3(b) and Fig. 4(a)) as it is already described before. In order to find a limit of thickness of the concrete cover, which potentially suppresses a spalling of the concrete cover.

As shown in Fig. 4(b) the failure of the specimens, which are reinforced with impregnated textile fabrics, tends strongly to take place near the clamped supports. The formation of longitudinal cracks is not as much pronounced compared to the yarn reinforcement. The failure is characterized by an extensive spalling of the concrete cover bounded by two orthogonal cracks resulting in the rupture of the impregnated textile. The appearance of spalling supports the hypothesis that the textile fabric acts as a separator and reduces the matrix strength in the out of plane direction. Besides, a different spalling pattern on both faces of the specimen can be observed leading to the assumption that the damage develops independently on both sides of the textile fabrics.

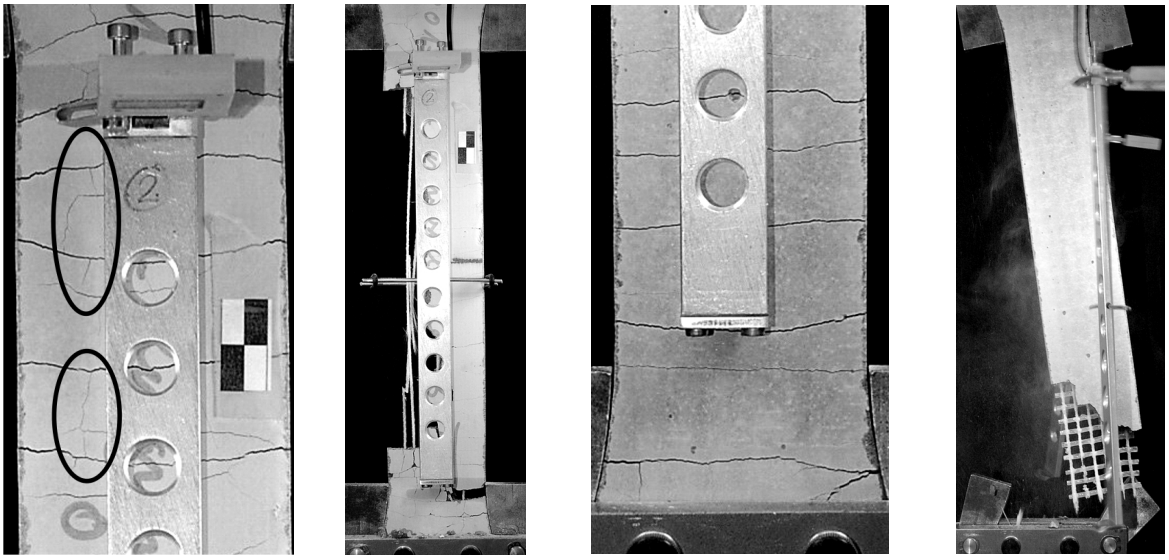

(a) Observed crack pattern (left) state of failure (right) series 3

(b) Observed crack pattern (left) state of failure (right) series 2

Fig 4: Observed crack pattern and state of failure of TSP specimens with a thickness of 10 mm

3 Modeling of the longitudinal crack development

3.1 Mechanical idealization of the spalling effect

The spalling effect observed also for steel-reinforced concrete has been explained by the accumulation of the circumferential stress around the reinforcement by Tepfers [7] (Fig. 5(b) left). He introduced the assumption of damage along the ring as shown in Fig. 5(a). An alternative assumption of plastic yielding within the tensile ring was presented by Martin [8] (Fig. 5(b) right). In the longitudinal direction both models derive the stress distribution from the mechanical bond between the reinforcement and matrix induced by the ribs (Fig. 6(a)).

The development of radial tensile stresses can then be explained through the three dimensional stress state developing from the rib being pulled-out from the matrix (Fig. 6(b)). There were several attempts to transfer those models, originally established for steel and FRP reinforcement, to fiber reinforcement [9, 10]. However, none of them supplied satisfactory results.

While the cited work is primarily focused on the steel reinforcement equipped with ribs, the impregnated yarns studied here have relatively smooth bond contact to the matrix and the stress transfer is solely due to a chemical bond and friction. Still, the performed tests evidently show that the ring stresses leading to longitudinal cracks develop also in this case.

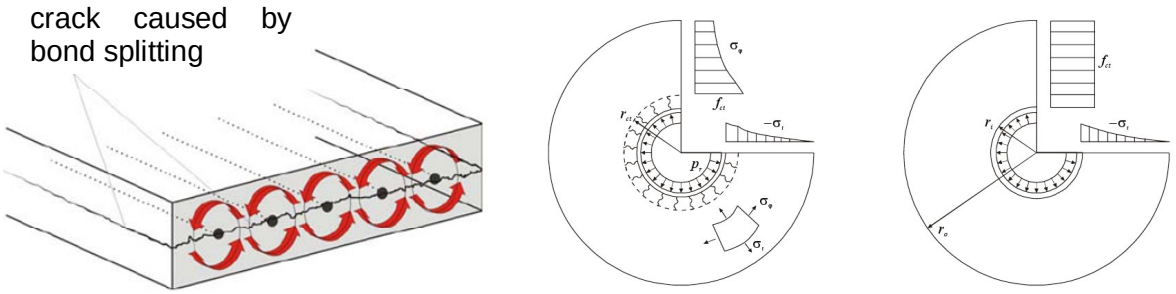

(a) (b)

Fig 5: (a) Superposed ring stresses causing the spalling of the concrete deck. (b) Models for the evaluation of the carrying capacity of the concrete in radial direction, left: Tepfers [7], right: Martin [8]

In order to illuminate the development of the ring stresses during the debonding process and to show the correspondence with the traditional models used for steel-reinforced concrete a detailed finite element simulation of the representative crack bridge was performed.

3.2 Representative crack bridge

The applied modeling approach exploits the periodicity of lateral cracks in the TSP-specimens. The presence of the periodic crack pattern, together with fact that the initiation of longitudinal cracks is more or less randomly distributed along the tensile specimen, allows us to apply the concept of a representative crack bridge. The idealization steps applied in the construction of the representative crack bridge are depicted in Fig. 7 (left). The imposed periodic boundary conditions can be summarized as follows:

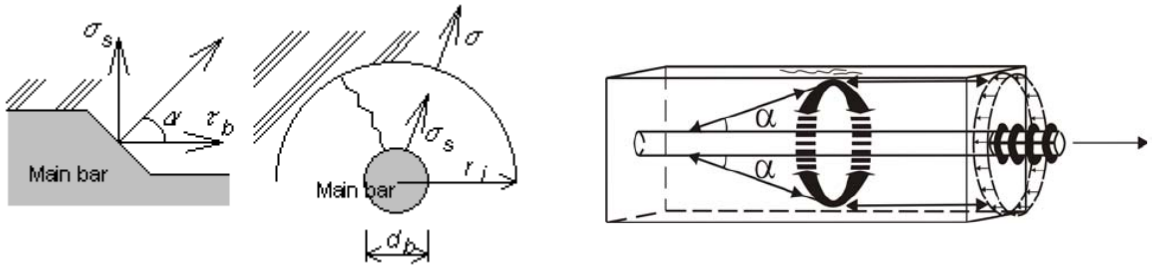

(a) (b)

Fig 6: (a) Radial stress state caused by the pull out of the rib [10]; (b) Model of the stress distribution [7]

- Displacement equality (in longitudinal direction) of the matrix and reinforcement can be assumed at the center of each concrete block between two crack planes. In order to reproduce the three dimensional stress state in the matrix, the overall displacement field can be regarded as relative to the displacement of the "plane of crack segment's symmetry" (see Fig. 8). Thus, zero displacement can be imposed for the plane of displacement equality.

- The periodic layout of reinforcing yarns in a cross-section can be used for further reduction of the model size. Zero displacement (in transverse direction) is also imposed in the symmetry plane between two neighboring rovings. The modeled region is depicted in the zoomed part of Fig. 7 (bottom left). The yarn was connected to the matrix via damage based bond model including both an adhesive and cohesive part [11]. A qualitative profile of the bond law is shown in Fig. 7 (top right). The calibration of the bond law was performed using pull out tests. Constitutive behavior of concrete was modeled using an anisotropic damage model of the microplane type [12]. The reinforcing yarn was represented as a homogeneous elastic bar.

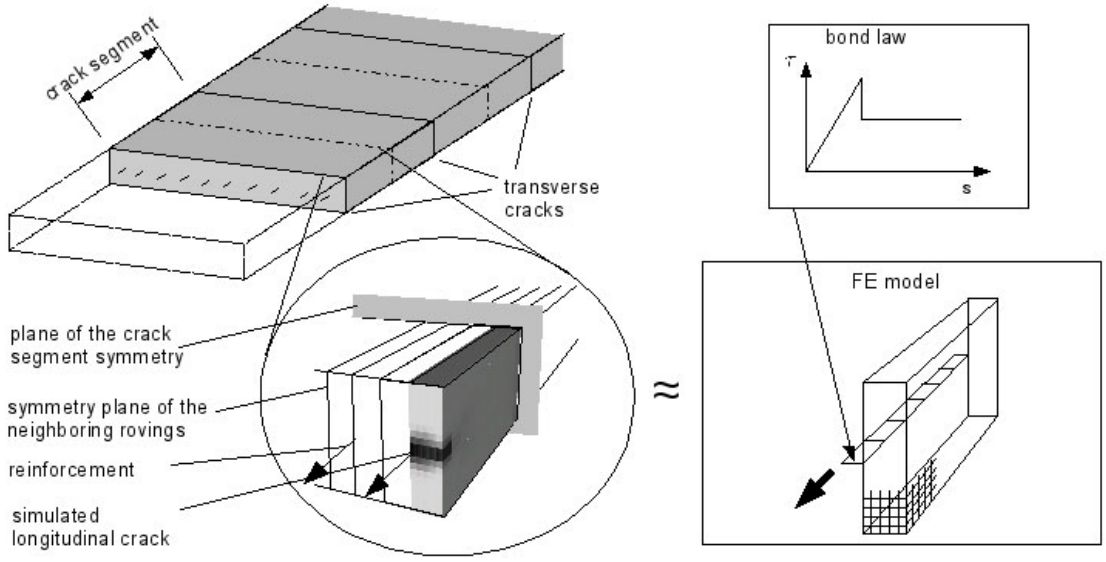

Fig. 7: Simulated localization of damage to a longitudinal crack (dark area) in tensile specimen on a periodic cell defined by the symmetries of the displacement and strain fields in the lateral and in the longitudinal direction

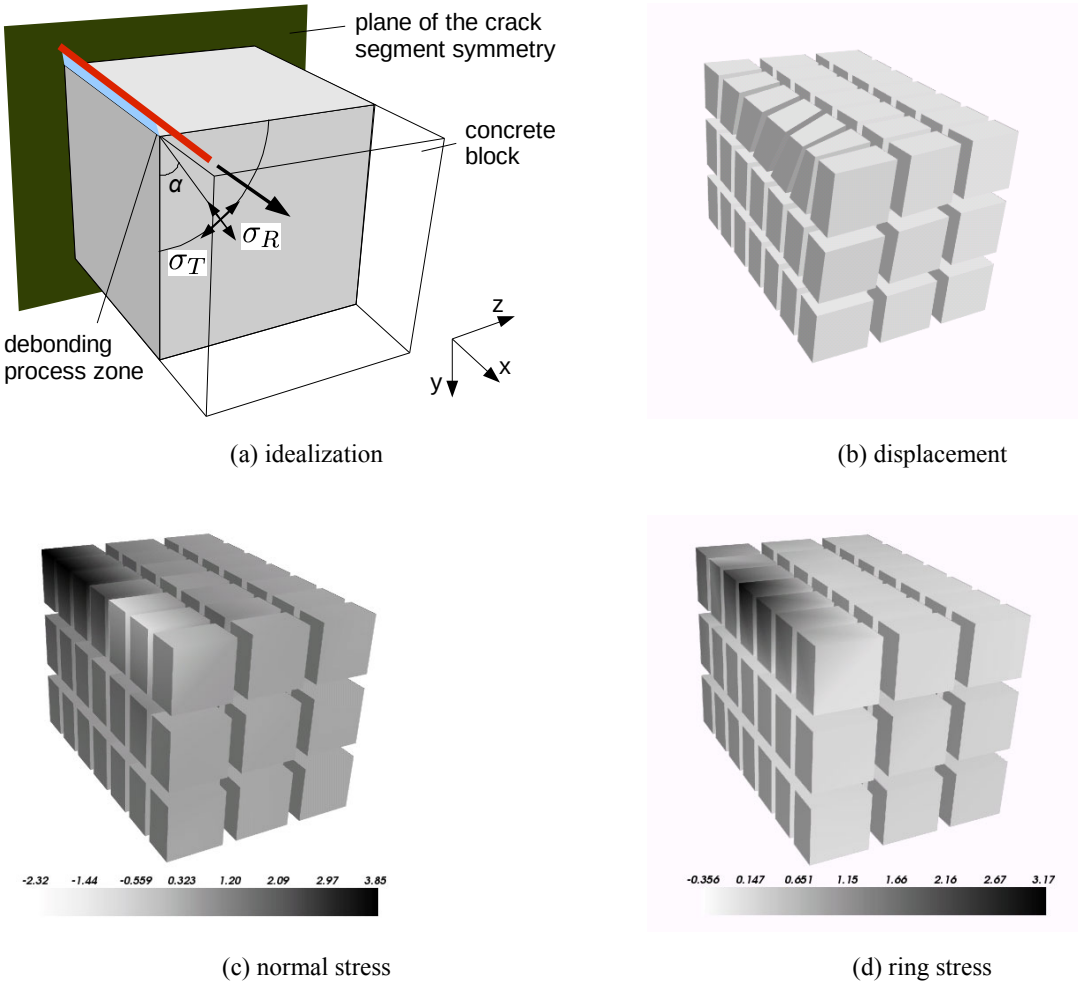

(a) idealization (b) displacement

(c) normal stress (d) ring stress

Fig. 8: Crack bridge idealization and simulated displacement-, normal stress- and ring stress distributions

The simulated development of damage within the representative crack bridge is shown in Fig. 7 (bottom). The dark color represents the localized damage that leads to the longitudinal macro crack oriented from the yarn to the nearest free surface. The performed qualitative numerical studies revealed the correspondence between the shape of the bond law shown in Fig. 7 (top right) and the development of the longitudinal cracks. The longitudinal crack occurs in connection with an abrupt drop from the adhesive to cohesive part of the bond law that leads to increased ring stresses in the vicinity of the debonding process zone.

For deeper insight into the development of tensile stresses leading to the longitudinal cracks it is helpful to visualize the three-dimensional stress state in the vicinity of the debonding process zone. For this purpose the crack bridge idealization shown in Fig. 8 has been used. Here, an additional plane of displacement symmetry above and below the roving was included. Fig. 8(a) shows the position of the reinforcement with respect to the concrete block in the stage of advanced debonding. The adhesive bond is available only in the part between the

debonding process zone and the plane of symmetry of the concrete segment (the backward y-z plane). Fig. 8(b) shows the displacement distribution of the matrix. Fig. 8(c) visualizes the stress distribution in the x-direction parallel to the reinforcement (the black color indicates the maximum tensile stresses).

Fig. 8(d) shows the distribution of the ring stresses around the reinforcement evaluated according to the top left figure. For each material point the ring projection of the stress tensor of the form $\sigma_T = n_i n_j \sigma_{ij}$ has been performed where $n_i = \{0, -\sin\alpha, \cos\alpha\}$ represents the tangent vector with respect to the ring and σ_{ij} is the three dimensional stress tensor. The angle α is measured from the y axis within the y-z plane. The dark color indicates that around the process zone, tensile ring stresses develop in a similar way as assumed for reinforcement with ribs described previously in Sec. 3.1. The simulation documents that no ribs are necessary for the development of high tensile ring stresses in the vicinity of the process zone.

Here, the tensile ring stresses develop due to the combined condition of (1) spatial layout of the material components with the given ratio of the bond and bulk stiffness (2) boundary conditions inducing rotationally symmetric stress state around the reinforcement and (3) the Poison's effect in the concrete matrix.

4 Conclusions

The spalling effect occurring under tensile loading of penetrated multi-filament yarns and textile fabrics has been studied both experimentally and numerically. The experimental study of the spalling effect has been performed with the goal to classify the damage mechanisms leading to the development of longitudinal cracks. The important goal was the design and identification of the test setup capable of rendering the longitudinal cracks under possibly uniform distribution of tensile stresses without any disturbing effect of the stress concentration near the clamping. For this purpose the use of TSP-specimens reinforced with impregnated yarns seems to be suitable more than these reinforced with impregnated textile fabrics.

The development of ring stresses in the vicinity of the debonding process zone has been reproduced using a strength based bond law with a distinguished adhesive and cohesive part. The resulting stress state is comparable with idealization of the three dimensional stress state based on the mechanical bond with ribs. However, the role of the ribs is played here by the adhesive process zone in the front of the developing mode II debonding crack. In the presented simulation the anisotropic damage model applied for the concrete could reproduce the development of a longitudinal crack. Thus, it can be regarded as feasible for detecting the combinations of component material parameters with a proneness to spalling. Further numerical studies shall provide more information about the possibilities how to delay or avoid the development of longitudinal cracks in order to exploit the full potential of the reinforcement's load carrying capacity.

5 Acknowledgements

This project is part of the research program ”SFB 532: Textile-Reinforced Concrete” of the German Research Foundation (DFG). The support is gratefully acknowledged.

6 References

[1] S. VOSS: *Ingenieurmodelle zum Tragverhalten von Textilbewehrtem Beton.* PhD., RWTH Aachen, Aachen (2008)

[2] SCHLESER M., WALK-LAUFFER, B., RAUPACH, M., DILTHEY, U.: Application of Poly mers to Textile-Reinforced Concrete, *Journal of Materials in Civil Engineering,* 18(5), 670-676 (2006)

[3] SJÖGREN, A., JOFFE, R., BERLUND, L., AND MÄDER, E.: Effects of Fibre Coating (Size) on Properties of Glass/Vinyl Ester Composite, *Composites, Part A: Applied Science and Manufactur, 30,* (1999)

[4] BRAMESHUBER, W.; BROCKMANN, T.; HEGGER J.; MOLTER, M.: Untersuchungen zum textilbewehrten Beton. *Beton 52* (2002) Nr.9, S. 424-429

[5] H. CUYPERS, J. WASTIELS: A stochastic matrix cracking theory for glass-fibre rein forced cementitious composites, *Materials and Structures,* Vol 39 (292), (2006)

[6] H. CUYPERS: *Analysis and Design of Sandwich Panels with Brittle Matrix Composite Faces for Building Applications.* PhD., Vrije Universiteit Brussel, Brussels (2002)

[7] R. TEPFERS: *A theory of bond applied to tensile reinforcement splices for deformed bars. PhD.*, Chalmers University of Technology, Götteborg (1973)

[8] H. MARTIN: *Zusammenhang zwischen Oberflächenbeschaffenheit, Verbund und Sprengwirkung von Bewehrungsstählen unter Kurzzeitbelastung.* Deutscher Ausschuss für Stahlbeton, Heft 228, Berlin(1973)

[9] R. TEPFERS, E. COSENZA, J. MODNIKS ET AL.: Bond of nonmetalic Reinforcement. In: *Task Group Bond Models fib (CEP-FIP), Bond of RC* (Bulletin 10),Stuttgart (2000)

[10] T. SAKAI, T KANAKUBO, K. YONEMARU ET AL.: Bond Splitting Behavior of Continuous Fiber Reinforced Concrete Members. In: *Fiber Reinforced Polymer for Reinforced Concrete Structures*, (1999)

[11] M. KONRAD: *Effect of multifilament yarn crack bridging on uniaxial behaviour of tex tile reinforced concrete*. PhD., RWTH Aachen, Aachen (2008)

[12] M. LEUKART, E. RAMM: An Alternative Split within the Microplane Material Model,. In Proceedings: *WCCM V FifthWorld Congress on Computational Mechanics* (2002)